

A Novel STFT Implementation for the Analysis of Non-Stationary Jammer Interference

Lutfiye Durak*, Orhan Arikan**, and Iickho Song*

* Department of Electrical Engineering
Korea Advanced Institute of Science and Technology
373-1 Guseong Dong, Yuseong Gu, Daejeon 305-701, Korea
lutfiye@Sejong.kaist.ac.kr, i.song@ieee.org

** Department of Electrical Engineering
Bilkent University
Ankara, 06800, Turkey
oarikan@ee.bilkent.edu.tr

ABSTRACT

A novel adaptive short-time Fourier transform (STFT) implementation for the analysis of non-stationary multi-component jammer signals is introduced. The proposed time-frequency distribution is the fusion of optimum STFTs of individual signal components that are based on the recently introduced generalized time-bandwidth product (GTBP) definition. The GTBP optimal STFTs of the components are combined through thresholding and obtaining the individual component support images, which are related with the corresponding GTBP optimal STFTs.

KEY WORDS

Non-stationary signal analysis, linear time-frequency distributions, short-time Fourier transform, generalized time-bandwidth product, multi-component chirp jammers.

1 Introduction

Spread spectrum techniques inherently provide resistance to jammer interference by the despreading gain. However, if the interference is much stronger than the desired signal, the gain becomes insufficient to decode the signal reliably. This is the case when interference stations are much closer to the receiver than the transmitter, or the transmitted signal is affected by fading. Therefore, in spread spectrum communications, several interference excision techniques are employed to improve the receiver performance and reduce the bit error rates including adaptive filtering, transform domain methods and time-frequency analysis techniques [1-4]. In particular, the non-stationary interference mitigation of chirp jammers is based on the time-frequency distributions of the short-time Fourier transformation (STFT) as in [3] or the Wigner distribution (WD) as in [1]. The chirp jammers have wideband frequency characteristics with narrow instantaneous bandwidth and the interference is suppressed once the jammer characteris-

tics are identified by using the time-frequency distributions. This is achieved either by masking out the jammer from the 2-D STFT followed by the synthesis of the jammer-free signal [3] or by adaptive time-varying filtering where the parameters of the interfering signal is estimated from the WD [5].

In both of these interference excision techniques, inherent drawbacks of the time-frequency distributions limit the system performance. An important criterion for the success of time-frequency representations is how well it preserves the time-frequency domain support of signals. Among the commonly used time-frequency representations, WD is the best in this respect. However, since the WD is a quadratic time-frequency distribution, in the case of multi-component signals, the cross-terms of the WD clutters the obtained time-frequency representation. Therefore, in a way it disturbs the actual support of the signal in the time-frequency domain. The linear STFT family provides time-frequency representations without cross-terms, but poor time-frequency localization of signal components is the major drawback of the STFT.

Recently, by investigating the effect of the STFT kernel on the time-frequency support of signal components, an optimal STFT implementation based on a novel generalized time-bandwidth product (GTBP) is proposed in [6]. The computationally efficient optimal STFT provides the most compact representation of single component signals considering their GTBP and yields optimally compact time-frequency supports for chirp signals on the STFT plane. In this paper, the GTBP optimal STFT implementation is extended for multi-component signals and it is proposed as a powerful analysis tool of spread spectrum communication applications in the presence of multi-component chirp jammers.

2 Time-Frequency Localization by STFT

The discrete STFT of a signal $x(t)$ is defined as¹ [7]

$$\begin{aligned} \text{STFT}_x(nT, mF) &= \int x(t')g^*(t' - nT)e^{-j2\pi mFt'} dt' \\ &\simeq T \sum_{n'} x(n'T)g^*(n'T - nT)e^{-j2\pi mFn'T}, \end{aligned} \quad (1)$$

where $g(\cdot)$ is the kernel function, n, m, n' are integers, and T and F are the sampling intervals of time and frequency. By using the FFT techniques, (1) can be implemented efficiently.

The choice of the STFT kernel $g(t)$ determines the time-frequency signal localization properties of the distribution. The Gaussian function is the most commonly used kernel function because it has the minimum time-bandwidth product (TBP), which is defined as

$$\text{TBP}\{x(t)\} = T_x \cdot B_x, \quad (2)$$

where T_x and B_x are the time-width and bandwidth of a signal $x(t)$. The TBP has been commonly used as a measure for the time-frequency domain support of the signal. The well-known uncertainty principle dictates that $1/(4\pi)$ is a lower bound on the TBP of a signal and only the Gaussian signal has a TBP that is equal to this lower bound [8].

For an STFT kernel function $g(t)$, the time-frequency domain support of the representation of a signal $x(t)$ can be zoned into a rectangular region with time and frequency dimensions $\sqrt{T_x^2 + T_g^2}$ and $\sqrt{B_x^2 + B_g^2}$, respectively [9]. Therefore, if the TBP is chosen as the measure of support, a well-defined optimization problem can be cast for the optimal STFT kernel, and the TBP optimal STFT kernel $g_{\text{TBP}}(t)$ is derived as [10]

$$g_{\text{TBP}}(t) = e^{-\pi t^2 B_x / T_x}. \quad (3)$$

To illustrate the improvement of the time-frequency localization of STFT due to the optimization of the window function with respect to the TBP, we compare the STFT of a chirp signal presented in Fig. 1. We have used two different kernel functions: One is the zeroth-order Hermite-Gaussian function $g(t) = e^{-\pi t^2}$ and the other is the TBP optimal STFT kernel (3) in Fig. 2 - (a) and (b), respectively.

However, the bounding rectangle of a signal support may be much larger than the signal support itself for signals whose frequency content varies by time as illustrated in Fig. 3 for a quadratically frequency modulated (FM) signal, as an example. Moreover, any time-frequency domain rotation operation that is implemented by the fractional Fourier transformation (FrFT) changes the TBP significantly. Even though the rotation operation does not change the area of the support of a signal, the TBP changes. The minimum TBP is reached when the signal support lies along the time or frequency axis. Therefore, the TBP is shown as an *upper*

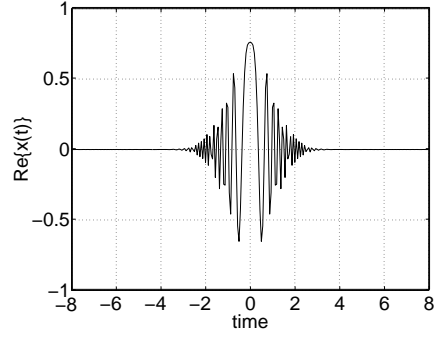


Figure 1. Time-domain representation of the chirp signal whose time-frequency domain localization by the STFT is compared in Fig. 2.

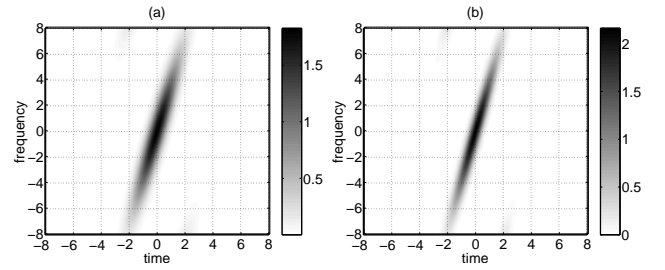


Figure 2. Time-frequency domain localization of the STFT by (a) the zeroth-order window function and (b) TBP optimal window function is compared. The TBP optimal STFT illustrated in (b) has a significantly improved time-frequency support than the STFT computed by zeroth-order Hermite-Gaussian window function illustrated in (a).

bound to the support of the signal in the time-frequency domain and a tighter measure of the support, called the ‘*generalized TBP (GTBP)*’, is defined as [6]

$$\text{GTBP}\{x(t)\} = \min_{0 \leq a < 4} \text{TBP}\{x_a(t)\}. \quad (4)$$

In (4), $x_a(t)$ is the a^{th} order fractional Fourier transformation (FrFT) of $x(t)$ given by [8, 11]

$$x_a(t) \equiv \{\mathcal{F}^a x\}(t) = \int B_a(t, t')x(t')dt' \quad (5)$$

with $a \in \mathbb{R}$, $0 < |a| < 2$ and the transformation kernel $B_a(t, t')$ is

$$\begin{aligned} B_a(t, t') &= \frac{e^{-j(\pi \text{sgn}(\sin \phi)/4 + \phi/2)}}{|\sin \phi|^{1/2}} \\ &\times e^{j\pi(t^2 \cot \phi - 2tt' \csc \phi + t'^2 \cot \phi)}. \end{aligned} \quad (6)$$

The FrFT is a generalization of the ordinary Fourier transform where the fractional order parameter a corresponds to the a^{th} power of the Fourier transform operator \mathcal{F} . The first-order FrFT is the ordinary Fourier transform and the zeroth-order FrFT is the function itself. The

¹All integrals are from $-\infty$ to $+\infty$ unless otherwise stated.

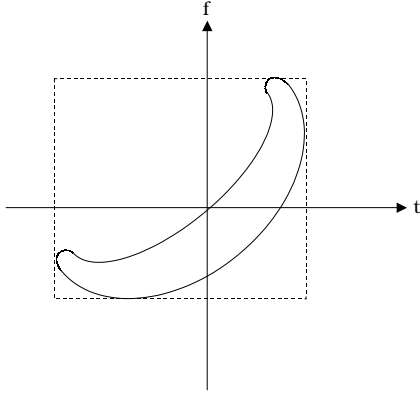


Figure 3. A TBP which is not usually a tight measure for the time-frequency support of signals.

a^{th} order FrFT interpolates between a function $x(t)$ and its Fourier transform $X(f)$. The continuous FrFT given by (5) can be approximated with discrete samples of $x(t)$ by using the fast computation algorithm proposed in [12] in $O(N \log N)$ operations.

As illustrated in Fig. 4, the GTBP provides the tightest bounding rectangle to the support of the signal in the time-frequency domain, hence providing a more representative support information than the TBP.

2.1 GTBP Optimal STFT of Single-Component Signals

As a consecutive step to the TBP optimal STFT, the optimal STFT kernel considering the GTBP of a single-component signal is analytically determined in [6]. For a signal $x(t)$ whose bounding rectangle is oriented at an angle ϕ_0 , which is not equal to 0 or $\pi/2$, the fractionally Fourier transformed signal $x_{a_0}(t)$ where $a_0 = \frac{2}{\pi}\phi_0$ has its bounding rectangle oriented along the time axis. For the transformed signal $x_{a_0}(t)$, the TBP and GTBP are the same. Therefore, for $x_{a_0}(t)$, the optimal STFT window is the Gaussian window given in (3) with $T_{x_{a_0}}$ and $B_{x_{a_0}}$ the corresponding time-width and bandwidth of the transformed signal, respectively. Then, the desired time-frequency representation of $x(t)$ is obtained by the counter-clockwise rotation of the optimal STFT for $x_{a_0}(t)$ by an angle of ϕ_0 .

Using the FrFT properties, the GTBP optimal distribution $D_x(nT, mF)$ is shown to have an ordinary STFT form

$$D_x(t, f) = e^{-j\pi\psi} \int x(t') g_{GTBP}^*(t' - nT) \cdot e^{-j2\pi mFt'} dt' \quad (7)$$

where $\psi = (t^2 - f^2) \sin \phi_0 \cos \phi_0 + 2tf \sin^2 \phi_0$, and the optimal kernel is

$$g_{GTBP}(\tau) = K e^{-j\pi\tau^2 \frac{\cot \phi_0 (\gamma^2 - 1)}{\gamma^2 + \cot^2 \phi_0}} e^{-\pi\tau^2 \frac{\gamma \csc^2 \phi_0}{\gamma^2 + \cot^2 \phi_0}} \quad (8)$$

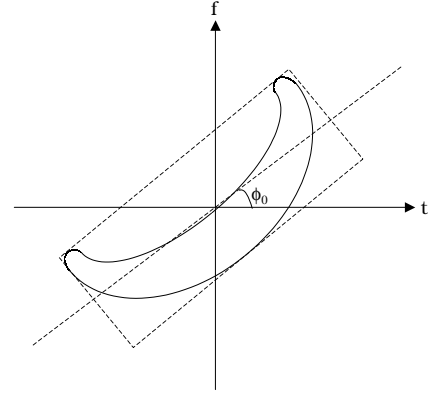


Figure 4. GTBP is the area of the tightest bounding rectangle to the support of the signal in the time-frequency domain, providing a better measure for the time-frequency domain signal supports.

where $K = \sqrt{(1 + j \cot \phi_0)/(\gamma + j \cot \phi_0)}$ and $\gamma = B_{x_{a_0}}/T_{x_{a_0}}$. In the evaluation of the GTBP optimal STFT, the fractional Fourier order parameter a_0 minimizing the TBPs and also the ratio of the corresponding bandwidth and time-width of the transformed signal should be determined.

The explicit form of the GTBP optimal STFT distribution in (7) provides significant practical savings in computation. Once the fractional order a_0 is determined, the computational complexity of (7) is the same as that of the ordinary STFT.

3 GTBP Optimal STFT Analysis of Multi-Component Signals

The GTBP optimal STFT analysis can be extended to the case of multi-component signals

$$x(t) = \sum_{k=1}^N x_k(t) \quad (9)$$

that are expressed as a linear combination of signals, including shifted and scaled Gaussian signals, chirps, or any higher-ordered FM signals. To obtain a well-localized time-frequency representation of a multi-component signal, the orientation of signal components on the time-frequency plane, and consequently the required FrFT order parameters should be determined. Following the GTBP optimal time-frequency analysis of each component, the individual representations are combined so that the time-frequency localization of each representation is optimally compact. In Section 3.1, the determination of signal adaptive parameters are explained. The fusion algorithm is described in Section 3.2.

3.1 Determination of Signal Adaptive Parameters

There are many alternative approaches to the determination of the optimal fractional Fourier order parameters a_k to be used in the GTBP optimal STFT analysis. Since the optimal fractional order a_k corresponding to a signal component and its orientation in the time-frequency plane are related by $\phi_k = a_k \frac{\pi}{2}$, the optimal order can be estimated by determining the orientation of the signal in the time-frequency plane. One way of determining the orientation of a signal in the time-frequency plane is to search for the peaks in the FrFT magnitudes computed at various fractional orders [13].

This method makes use of the relationship between the Radon-Wigner transform (RWT) of a signal and its FrFT [8]. The RWT of a function $x(t)$ is defined as the Radon transform of the WD of $x(t)$ as

$$RDN[W_x](r, \phi) = \int W_x(r \cos \phi - s \sin \phi, r \sin \phi + s \cos \phi) ds \quad (10)$$

where (r, ϕ) are the transform domain variables in polar format. The RWT gives the projection of the WD for $0 \leq \phi \leq \pi$. It has been shown in [8] that the radial slices of the RWT, or equivalently $RDN[W_x](r, \phi)$, can be directly computed from $x(t)$ by

$$\begin{aligned} RDN[W_x](r, \phi) &= |\{\mathcal{F}^a(x)\}(r)|^2 \\ &= |x_a(r)|^2 \end{aligned} \quad (11)$$

where $RDN[W_x](r, \phi)$ is the ϕ -Radon projection of the WD given in (10) and $x_a(r)$ is the a^{th} order FrFT of the signal defined by (5).

By searching peaks of $|x_a(r)|^2$ computed at various values of the fractional order a , the orientation of the signal supports are estimated robustly for single component signals in [6]. For multi-component signals, the estimates of the orientation angles can be automatically detected by searching the peaks using a sliding window. In practice, it is sufficient to determine the angle of the orientation angle of the signal supports in a moderately large neighborhood of the exact angle. This is because it has been shown in [6] that the spread of the signal components changes slowly as the FrFT order approaches the optimum value. This provides the determination of the optimal FrFT order parameter determination procedure robust to small angle changes as far as the time-frequency localization is concerned. In practice, search for the optimal fractional order can be conducted approximately by computing the FrFT of the signal at 10 to 30 different fractional orders. Since each FrFT computation is of $O(N \log N)$, the overall complexity of the required search is also of $O(N \log N)$.

The search algorithm for the orientation angles of the components is illustrated for a two-component signal embedded in additive Gaussian noise with an SNR level of 5 dB in Fig. 5. The STFT of the signal with a zeroth-order Hermite-Gaussian kernel function is presented in Fig. 6. The projection analysis using the FrFT presented in

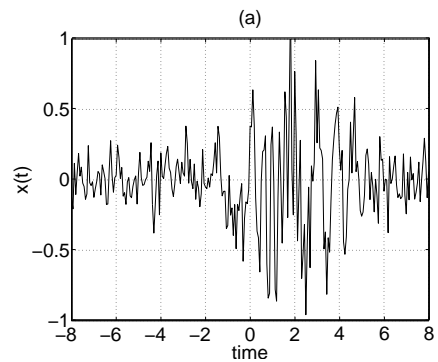


Figure 5. A two-component signal embedded in additive Gaussian noise with an SNR level of 5 dB.

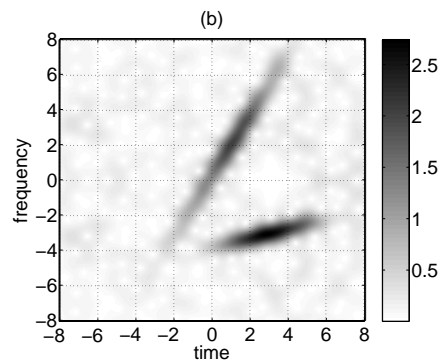


Figure 6. The STFT of the two-component signal with a zeroth-order Hermite-Gaussian STFT kernel.

Fig. 7 indicates the orientation angles of both signal components at $\phi = 15^\circ$ and $\phi = 60^\circ$.

3.2 Fusion Algorithm

Following the determination of the N orientation angles ϕ_k for all $1 \leq k \leq N$, and estimating the corresponding FrFT domain spreads of each component, a number of N GTBP optimal STFTs are computed using (7). The individual optimal STFTs of the simulation example is presented in Fig. 8.

The methods of automatic fusion of individual GTBPs may vary depending on applications. If signal components are expected to have comparable energy content, then the supports of signal components can be determined through thresholding the individual distributions by choosing a threshold value as 10% of the maximum value of the corresponding GTBP optimal STFTs (shown in Fig. 8). The thresholding generates the images of supports as illustrated in Fig. 9 by taking value 1 for regions exceeding the threshold and 0 for the remaining. Then, a logical 'and' operation is performed over individual support images yielding compact supports for signal components $x_k(t)$ as shown in Fig. 10.

Finally, the components corresponding to the final

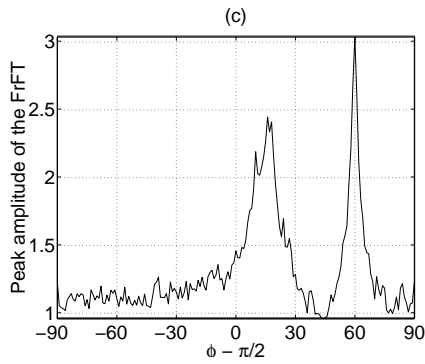


Figure 7. By searching peaks of the $|x_a(r)|^2$ signals computed at various a values, the orientation of the signal supports can be estimated robustly. The projection analysis using the FrFT is presented indicating the orientation angles of both signal components at $\phi = 15^\circ$ and $\phi = 60^\circ$.

supports can be matched to the individual GTBP optimal STFTs by taking into account of the component energy encapsulated by the support. In Fig. 10(a) and (b), the final support and the resultant adaptive STFT is presented. Alternatively, watershed segmentation algorithm can be used in the automatic determination of the supports of individual components [14].

The time-frequency localization of each signal component is significantly improved compared to the STFT in Fig. 6. In spread spectrum communication applications, the interference excision can be performed by masking out the high-power jammer signal supports and synthesize the jammer-free signal from the remaining time-frequency distribution.

4 Conclusion

In this paper, the recently developed optimal STFT implementation based on the minimum TBP is extended to signals with multi-components. The GTBP optimal STFT analysis of each signal component provides a significant improvement for the time-frequency localization compared to the ordinary STFT analysis with a similar computational complexity.

The proposed GTBP optimal STFT of multi-component signals requires the determination of the parameters of individual signal components. In practical applications, these parameters should be adaptively chosen and comparison of the performances of alternative ways of determining these parameters requires further investigation.

Compared to the previously developed STFT-based interference excision system in [3], the proposed adaptive STFT is computationally efficient. Additionally, compared to the WD based higher-order time-frequency distributions, which retain cross-terms, this algorithm is robust. Therefore, it can be implemented in the interference excision techniques in the presence of multi-component jammers.

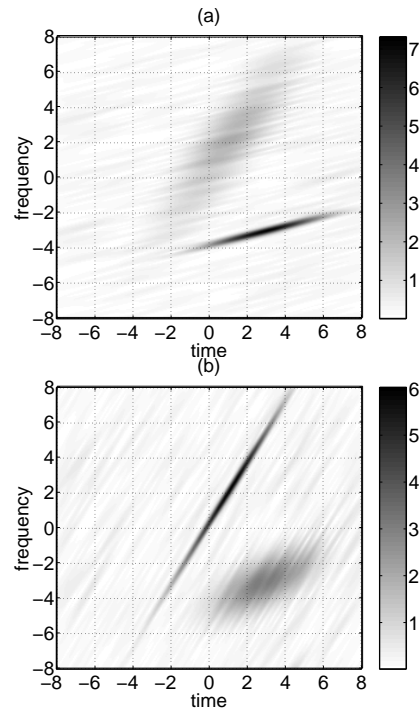


Figure 8. GTBP optimal STFTs associated with each signal component of the signal illustrated in Fig. 5.

Acknowledgement

This research was supported by Brain Korea 21 Project under a 2004 grant from the School of Information Technology, KAIST, for which the authors would like to express their thanks.

References

- [1] M. G. Amin, "Interference mitigation in spread spectrum communication systems using time-frequency distributions," *IEEE Trans. Signal Process.*, vol. 45, pp. 90–101, Jan. 1997.
- [2] J. Laster and J. Reed, "Interference rejection in digital wireless communication," *IEEE Signal Process. Magazine*, vol. 14, pp. 37–62, May 1997.
- [3] X. Ouyang and M. G. Amin, "Short-time Fourier transform receiver for nonstationary interference excision in direct sequence spread spectrum communications," *IEEE Trans. Signal Process.*, vol. 49, pp. 851–863, Apr. 2001.
- [4] J. Yuan and J. Lee, "Narrow-band interference rejection in DS/CDMA systems using adaptive (QRD-LSL)-Based Nonlinear ACM Interpolators," *IEEE Trans. Vehicular Tech.*, vol. 52, pp. 374–379, May 2003.

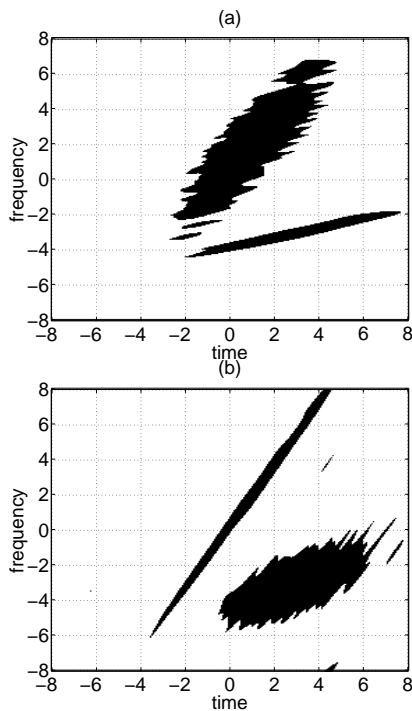


Figure 9. The supports of the signal components can be determined through thresholding the individual distributions by choosing a threshold value as 10% of the maximum value of the corresponding GTBP optimal STFTs illustrated in Fig. 8. Thresholding generates the images of supports by taking value 1 for regions exceeding the threshold and 0 for the remaining.

- [5] S. Barbarossa and A. Scaglione, "Adaptive time-varying cancellation of wideband interferences in spread-spectrum communications based on time-frequency distributions," *IEEE Trans. Signal Process.*, vol. 47, pp. 957–965, Apr. 1999.
- [6] L. Durak and O. Arıkan, "Short-time Fourier Transform: Two fundamental properties and an optimal implementation," *IEEE Trans. Signal Process.*, vol. 51, pp. 1231–1242, May 2003.
- [7] F. Hlawatsch and G. F. Boudreaux-Bartels, "Linear and quadratic time–frequency signal representations," *IEEE Signal Process. Magazine*, vol. 9, pp. 21–67, Apr. 1992.
- [8] H. M. Ozaktas, Z. Zalevsky, and M. A. Kutay, *The Fractional Fourier Transform with Applications in Optics and Signal Processing*, John Wiley & Sons, 2000.
- [9] L. Cohen, *Time–Frequency Analysis*, Prentice Hall, 1995.
- [10] L. Durak and O. Arıkan, "Generalized time-bandwidth product optimal short-time Fourier transformation," *Proc. IEEE Int. Conf. Acoust. Speech,*

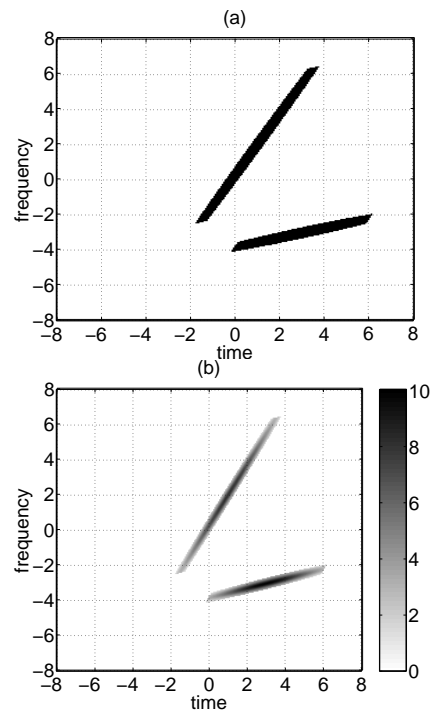


Figure 10. Fusion of the individual GTBP optimal STFTs of multi-component signals. In (a), a logical 'and' operation is performed over individual support images yielding compact supports for each signal component. Finally, in (b) the components corresponding to the final supports are matched to the individual optimal STFTs

- Signal Process.*, Orlando, USA, vol. 2, pp. 1465–1468, May 2002.
- [11] V. Namias, "The fractional order Fourier transform and its application to quantum mechanics," *J. Inst. Math. Appl.*, vol. 25, pp. 241–265, 1980.
- [12] H. M. Ozaktas, O. Arıkan, M. A. Kutay, and G. Bozdagi, "Digital computation of the fractional Fourier transform," *IEEE Trans. Signal Process.*, vol. 44, pp. 2141–2150, Sept. 1996.
- [13] A. W. Lohmann and B. H. Soffer, "Relationships between the Radon–Wigner and fractional Fourier transforms," *J. Opt. Soc. Am. A*, vol. 11, pp. 1798–1801, June 1994.
- [14] L. Vincent and P. Soille, "Watersheds in digital spaces: An efficient algorithm based on immersion simulations," *IEEE Trans. Pattern Analysis, Machine Intelligence*, vol. 13, pp. 583–598, June 1991.